

Microwave absorption properties of Co-La doped M-type Ba-Sr hexagonal ferrites in X-band

S. GUJRAL^a, K. S. BHATIA^b, H. SINGH^c, H. KAUR^{c,*}, N. GUPTA^d

^aIKGPTU, Department of Research and Development, Research Scholar, Jalandhar, India

^bG.B. Pant Institute of Engineering & Technology, Department of ECE, Associate Professor, Pauri Garhwal-246194, Uttarakhand, India

^cIKGPTU, CTIEMT Shahpur, Jalandhar, Department of ECE, Associate Professor Punjab, India

^dLyallpur Khalsa College of Engineering, Department of ECE, Assistant Professor, Jalandhar, India

In present research, we investigate microwave absorption properties of M-type hexagonal ferrite $\text{Ba}_{0.5}\text{Sr}_{0.5}\text{Co}_x\text{La}_x\text{Fe}_{12-2x}\text{O}_{19}$ ($0.0 \leq x \leq 1.0$; $x = 0.2$) compositions in X band developed using ceramic technique. Energy dispersive spectroscopy (EDS) spectra of different compositions are examined for composition details in frequency region (8.2-12.4) GHz. The doping of Co^{2+} and La^{3+} materials increase microwave frequency absorption, absorption bandwidth, reduces thickness & promotes impedance matching. Then, Scanning electron micrograph (SEM) confirm grain size adhere to microwave frequency absorption. The best reflection loss value of -43.73 dB is found with composition $x=0.2$, 1.9 mm thickness and at 10.75 GHz frequency.

(Received September 25, 2020; accepted August 16, 2021)

Keywords: Microwave absorption, Hexagonal ferrite, Scanning electron micrograph (SEM), Vector network analyzer (VNA)

1. Introduction

In present world, electromagnetic interference (EMI) is generated by enormous advancement of high-frequency devices that are utilized in the microwave frequency region such as Wi-Fi, WIMAX, ad-hoc networks, military, satellite communication, microwave devices, and RADAR [1-4]. This has inspired the investigators to find the microwave attenuating/absorbing constituents to impede the electromagnetic interference. There is maximum utilization of M-type hexagonal ferrites as microwave frequency absorbers because of their small density, good chemical strength, acceptable electrical resistivity, and less synthesis cost [5-7].

The investigation of reports is accessible regarding microwave attenuation/absorption properties of ferrite materials concerned with electromagnetic properties. Topkaya [8] suggested the magnetic and structural properties and temperature effects of barium hexaferrite (M-type) with the addition of doping ions Bi-La in $\text{BaBi}_x\text{La}_x\text{Fe}_{(12-2x)}\text{O}_{19}$ composition. This composition found enhanced saturation magnetization, coercivity field, and constant of effective anisotropy field with values 10 & 300K. Also, it was observed that the resonance field was enhanced with doping. Mortazavinik [9] explained the substitution of Zr^{2+} , Zr^{4+} , and Co^{2+} to synthesize M-type strontium hexagonal ferrite. It has given minimum reflection loss (RL) of -20 dB at frequency of 10.1 GHz and 90% bandwidth absorption of 3.5 GHz. Padhy [10] proposed U shape barium hexagonal ferrite with multilayer sample and Co-Cr doping ions which observed reflection loss (RL) of -80.94 dB with 1.801 mm thickness and bandwidth of 3.948 GHz. Arora and Narang [11]

investigated effects of $\text{Ba}_{(1-2x)}\text{La}_x\text{Na}_x\text{Fe}_{10}\text{CoTiO}_{19}$ barium hexagonal ferrite with the addition of Lanthanum and Sodium ions and found a reduction in unit cell volume and dc resistivity with doping. Also, it was informed that dielectric constant and tangent loss were enhanced at low-frequency region and then decreased for other range of frequencies. Further, Liu et al. [12] suggested the mono/dual layer composition of CNZF ferrite and NIO doping ions, the author concluded that reflection loss of -67 dB found at a frequency of 9.2 GHz. Also, absorption bandwidth (-10 dB) of 3.9 GHz was determined, where double layer absorber was found best to achieve microwave absorption. Also, Araz and Zenc [13] recommended barium hexagonal ferrite ($\text{BaFe}_{11}\text{CoO}_{19}$) with cobalt doping and toroid shape using the ceramic method in 2-18 GHz and obtained RL of -20 dB. Moreover, the author referred designed absorber to be suitable microwave absorber in the wideband frequency range. Septiani et al. [14] proposed M-type Sr hexagonal ferrite with substitution of Co/Ti ions and observed reduction in coercivity and also found absorption bandwidth of 13 GHz for compositions $x=0.3, 0.5$, and 1. Intaphong et al. [15] mentioned to synthesize nickel ferrite (NiFe_2O_4) by using iron, iron oxide, nickel oxide, and sodium perchlorate and concluded enhanced exothermicity, rough octahedron materials of approximately 500 nm along with saturation magnetization of 58.93 emu/g. Then, Dubey et al. [16] revealed magnetic properties and microwave effects of U type hexaferrite ($\text{Ba}_4\text{Mn}_2\text{Fe}_{36-2x}\text{Zn}_x\text{Ti}_x\text{O}_{60}$) by substituting Zn and Ti elements. The author provided RL of -30.9 dB with 99.9 % absorption at frequency of 11.9 GHz with $x=2.0$ and also $\text{RL} < -10$ dB with nearly 4.5 GHz bandwidth along

with 90% microwave absorption for $x=3.0$. You et al. [17] proposed Y type Ba hexagonal ferrite ($\text{Ba}_2\text{Fe}_{2-x}\text{Zn}_x\text{Fe}_{12}\text{O}_{22}$) with Zn^{2+} and Fe^{2+} substitutes and investigated RL of -50 dB with sample thickness of (1.52-1.80) mm and also observed increased permittivity with better impedance matching. Azizi et al. [18] synthesized material with Sr ferrite and doping of CFO ions. The author got absorption bandwidth of -8.1 dB at a frequency of 10.1 GHz by SrW/CFO powder and RL of -16.5 dB at a frequency of 9.7 GHz with frequency bandwidth of 3.53 GHz at thickness of 3.3 mm. Furthermore, Shelar and Yadav [19] examined properties of synthesized nickel-cadmium ferrite (Ni-Cd) and found saturation magnetization of 56 emu/g with $x=0.6$, the variation of complex permittivity (10-30) in the frequency range of 8-12 GHz and microwave absorption of 0.958 at frequency of 9.5 GHz with $x=0.6$. Also, Peymanfar [20] suggested the preparation of multi carbon nanotubes and ferrite $\text{Zn}_{0.25}\text{Co}_{0.75}\text{Fe}_2\text{O}_4$. It was concluded that absorption of 79.08 dB was achieved at a frequency of 10.5 GHz and thickness of 2.4 mm with bandwidth > 2.7 GHz. Kiseleva et al. [21] described the synthesized magnesium ferrite with polyethylene and found increased dispersion. Trukhanov et al. [22] examined properties of barium hexagonal ferrite $\text{Ba}(\text{Fe}_{1-x}\text{Sc}_x)\text{O}_{19}$ with Sc substitute and for x is ≤ 0.1 . It was concluded that maximum correlation was achieved between Sc^{3+} doping and diamagnetic ions and presented suitability of material in high frequency region. Moreover, Dhruv et al. [23] investigated properties of Z type strontium hexagonal ferrite with addition of gallium ions and observed permeability of (1-4) in X-band. Jafarian et al. [24] suggested polypyrrol precipitation with the addition of Cu ions and observed RL of -22 dB at matching frequency of 10.75 GHz. Kaur et al. [25] prepared M-type hexagonal ferrite $\text{Ba}_{0.5}\text{Sr}_{0.5}\text{Co}_x\text{In}_x\text{Fe}_{12-2x}\text{O}_{19}$ with addition of Co^{2+} and In^{3+} . It was investigated that RL of -39.99 dB was found with $x=0.2$, at a frequency of 11.14 GHz, and sample thickness of 1.6 mm. Garg et al. [26] recommended synthesizing strontium hexaferrite with titanium carbide and demonstrated high saturated magnetization of 45.1 emu/g, the low value of coercivity (255.09 G), reflection loss of -39.67 dB at 9.46 GHz with 2mm sample thickness and bandwidth of 2.77 GHz. Afshar et al. [27] prepared strontium hexaferrite and spinel ferrite and investigated RL of -14.5 dB at frequency of 9.5 GHz. Kaur et al. [28] proposed the composition of M-type strontium hexaferrite ($\text{Sr}_{1-y}\text{La}_y\text{Fe}_{12}\text{O}_{19}$) with doping of lanthanum material and examined best RL of -30 dB with absorption bandwidth of 2 GHz for composition 0.25 in K frequency band. Then, maximum absorption of 3.43 GHz was achieved in the Ka frequency region. Further, Fathi et al. [29] suggested the preparation of ferrite $\text{SrFe}_{12}\text{O}_{19}/\text{ZnFe}_2\text{O}_4$ and found RL of -30 dB at a frequency of 9.8 GHz. Later, Anh & Dan [30] prepared zinc-nickel $\text{Zn}_{0.8}\text{Ni}_{0.2}\text{Fe}_2\text{O}_4$ with SiO_2 and verified properties of designed sample in X-band. It was investigated that absorption of -20.74 dB was obtained at frequency of 10 GHz with 1.5 wt% sample weight.

With this motivation, we have prepared M-type hexagonal ferrite $\text{Ba}_{0.5}\text{Sr}_{0.5}\text{Co}_x\text{La}_x\text{Fe}_{12-2x}\text{O}_{19}$ samples and

examined the microwave absorption concerning the addition of doping ions Co^{2+} and La^{3+} in microwave frequency region 8.2 GHz to 12.4 GHz at temperature 1150 °C [31] and now in this paper results are extended for the same composition at temperature 1100 °C. To find microwave absorption because of loss tangents and their dependency with impedance matching mechanism is described. The examined condition for best microwave absorption can be represented as $|Z_{in}| = Z_0 = 377\Omega$, (where input impedance is represented by Z_{in} and characteristic impedance is represented by Z_0). Besides that dependency of quarter wavelength criterion is discussed in detail which is also a very prominent reason for absorption to occur.

2. Experimental procedure

M-type hexagonal ferrite $\text{Ba}_{0.5}\text{Sr}_{0.5}\text{Co}_x\text{La}_x\text{Fe}_{12-2x}\text{O}_{19}$ was prepared by standard ceramic method with composition ($0.0 \leq x \leq 1.0$ with steps of $x=0.2$). Different materials as La_2O_3 , CoCO_3 , SrCO_3 , BaCO_3 , and SrCO_3 of sigma Aldrich with purity 99.98 % were considered initially to make a composition. According to the chemical equation, the ratio of distinct materials of compositions is mixed in agate and pestle mortar with distilled water for eight hours and then grounded with the attached grinder to obtain a uniform mixture. Afterward, the pre-sintering of ground powders was done for ten hours at a temperature of 1000°C in a microcontroller-based electric furnace. Again grinding was performed with similar conditions to obtain refined powder. Then, sieves with mesh size of 220 B.S.S. were used to sieve powders. Thus, the required form of powders of hexagonal ferrite $\text{Ba}_{0.5}\text{Sr}_{0.5}\text{Co}_x\text{La}_x\text{Fe}_{12-2x}\text{O}_{19}$ were developed with composition ($0.0 \leq x \leq 1.0$ with steps of $x=0.2$). Later, rectangular-shaped pallets with size $0.0266\text{m} \times 0.01016\text{m}$ were prepared from powders by applying uniaxial pressure of 75 KN/m² with hydraulic press. Next, end sintering was achieved at a temperature of 1100 °C for fifteen hours and gently made cool identical to room temperature (by maintenance of cooled down rates to $\pm 5^\circ\text{C}$).

The respective compositions with their atomic and weight percentage were recorded using Energy dispersive spectra (EDAX) of the typical compositions ($x = 0.0, 0.2, 0.4, 0.6, 0.8$ and 1.0). Scanning electron microscopy (SEM) was adopted with model number D-8571 to study grain morphology. A rectangular waveguide was used with internal dimensions of $0.0286 \times 0.01016 \text{ m}^2$ where compositions were placed, which was then connected to VNA (Agilent model no. N5225A). S-parameters were analyzed using VNA to derive complex permittivity & complex permeability of material compositions in frequency region 8.2GHz -12.4 GHz: expression of complex permittivity $\epsilon_r = \epsilon' - j\epsilon''$ and complex permeability $\mu_r = \mu' - j\mu''$ where ϵ' is permittivity, ϵ'' is dielectric loss, μ' is permeability and μ'' is magnetic loss. Before analyzing actual measurements, the evaluation of the network analyzer was achieved in an air medium. The 90% and 99% power absorptions of material were represented by

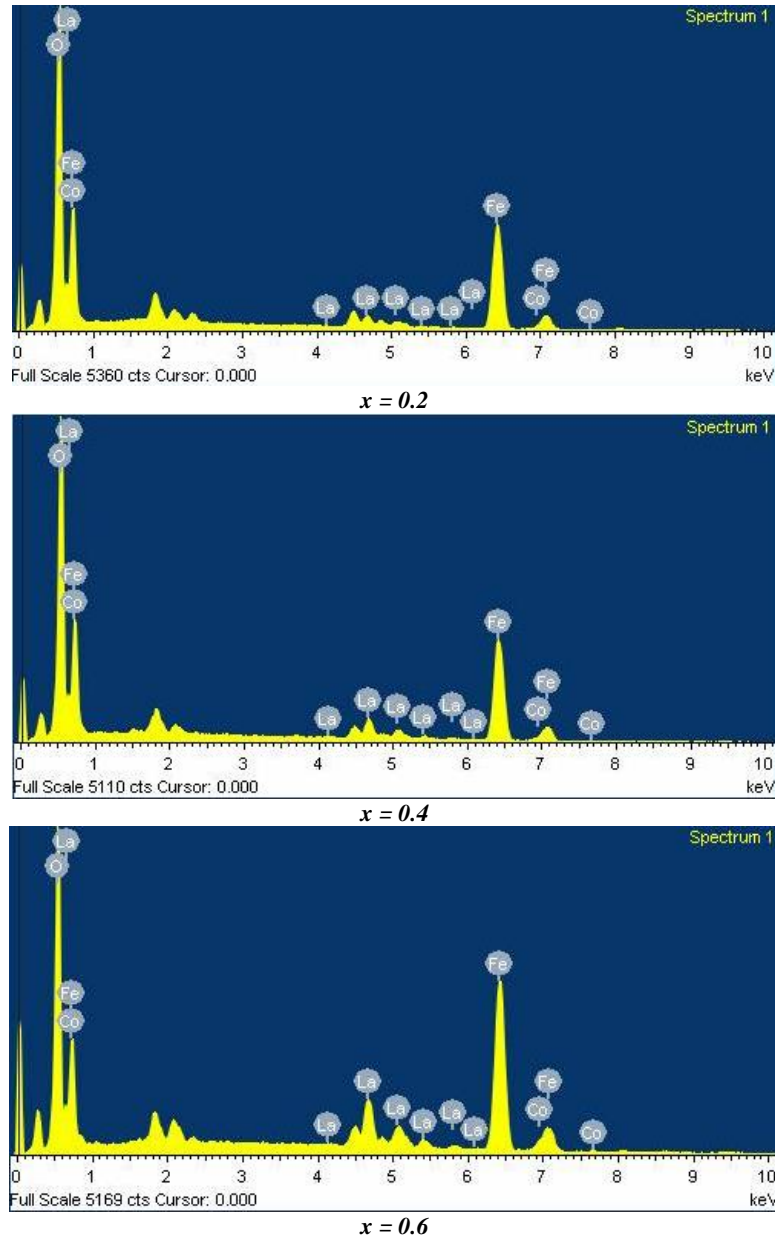
-10 dB reflection loss (RL) and -20 dB reflection losses.

Manuscript used different abbreviations and symbols which are Reflection loss (RL), Permittivity (ϵ'), Permeability (μ'), dielectric loss (ϵ''), Magnetic loss (μ''), Dielectric loss tangent ($\tan\delta_\epsilon$), Magnetic loss tangent ($\tan\delta_\mu$), Simulated thickness (t_{sim}) and Calculated thickness (t_{cal}).

3. Results with discussion

3.1. Structural and morphological analysis

The availability of various elements in the chemical composition of $Ba_{0.5}Sr_{0.5}Co_xLa_{12-2x}O_{19}$ hexagonal ferrites along with their elemental percentage was examined by the energy dispersive spectra (EDAX) of the typical compositions ($x = 0.2, 0.4, 0.6, 0.8$ and 1.0). These EDAX spectra of all samples are shown in Fig. 1.



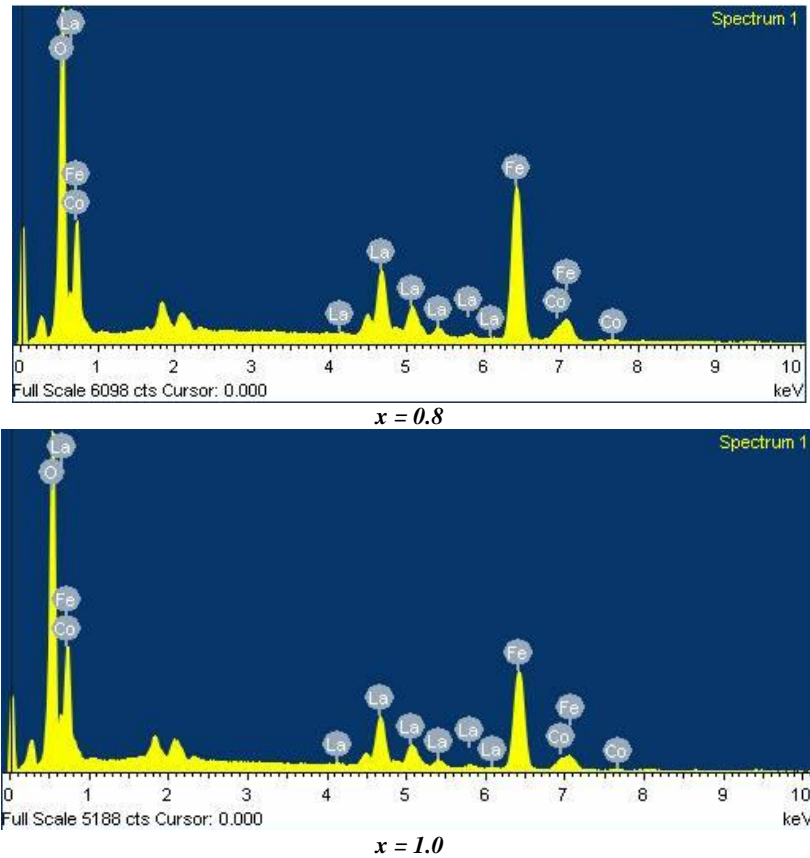


Fig. 1. Energy dispersive spectroscopy spectra of $Ba_{0.5}Sr_{0.5}Co_xLa_xFe_{12-2x}O_{19}$ ($x = 0.2, 0.4, 0.6, 0.8$ and 1.0) hexagonal ferrite (color online)

Table 1. Elemental composition weight & atomic percentage of typical samples of $Ba_{0.5}Sr_{0.5}Co_xLa_xFe_{12-2x}O_{19}$ ($x = 0.2, 0.4, 0.6, 0.8$ and 1.0) hexagonal ferrites

Element	Weight %	Atomic %								
	0.2		0.4		0.6		0.8		1.0	
O	33.83	65.05	32.29	64.70	21.63	52.51	21.84	54.21	28.22	63.07
Fe	60.45	33.30	55.57	31.89	58.40	40.61	51.35	36.51	43.20	27.66
Co	1.29	0.68	1.95	1.06	3.45	2.27	4.19	2.82	5.49	3.33
La	4.43	0.98	10.18	2.35	16.52	4.62	22.62	6.46	23.10	5.95
Total	100%		100%		100%		100%		100%	

The peaks of O, Fe, La, Co appear in the Energy dispersive spectroscopy spectra of $Ba_{0.5}Sr_{0.5}Co_xLa_xFe_{12-2x}O_{19}$ for all compositions. The observed chemical composition data comprising the weight ratio and atomic weight ratios as observed from EDAX are also mentioned in Table 1.

Fig. 2 represents the scanning electron micrographs of defined material compositions. The formation of large grains because of fusing of distinct crystallites is represented with composition $x=0.0$ and doped materials Co^{2+} & La^{3+} cause variation in size of grain. Some compositions $x=0.0, x=0.4$ and $x=0.6$ represented group

and agglomerated grains and compositions $x=0.8, x=1.0$ provided platelet-form grains. The group grain size is observed to be reduced with doping despite maximum ionic radii of doped Co^{2+} & La^{3+} cations compared to Fe^{3+} ions, so doping developed grain expansion.

3.2. Dynamic properties (dependent on frequency)

3.2.1. Complex permittivity and complex permeability

The changes which are observed in dielectric constant, dielectric loss, permeability, and magnetic loss which are represented by symbols ϵ' , ϵ'' , μ' and μ'' respectively with the composition ($0.0 \leq x \leq 0.6$ with steps of $x=0.2$) with respect to frequency are shown in Fig. 3. Different peaks

at all compositions are seen in the frequency regime of 8.4 to 12.4 GHz. The undoped composition $x=0.0$ has minimum values of ϵ' , ϵ'' with many-peaks throughout the frequency range. There is an increase in dielectric constant with the doping of Co^{2+} and La^{3+} , however, ϵ' , ϵ'' remains high in $x=0.2$. The dipole polarity controls ϵ' at the examined microwave frequency range and examined high values in ϵ'' developed from reduction concerned to the polarization of dipole.

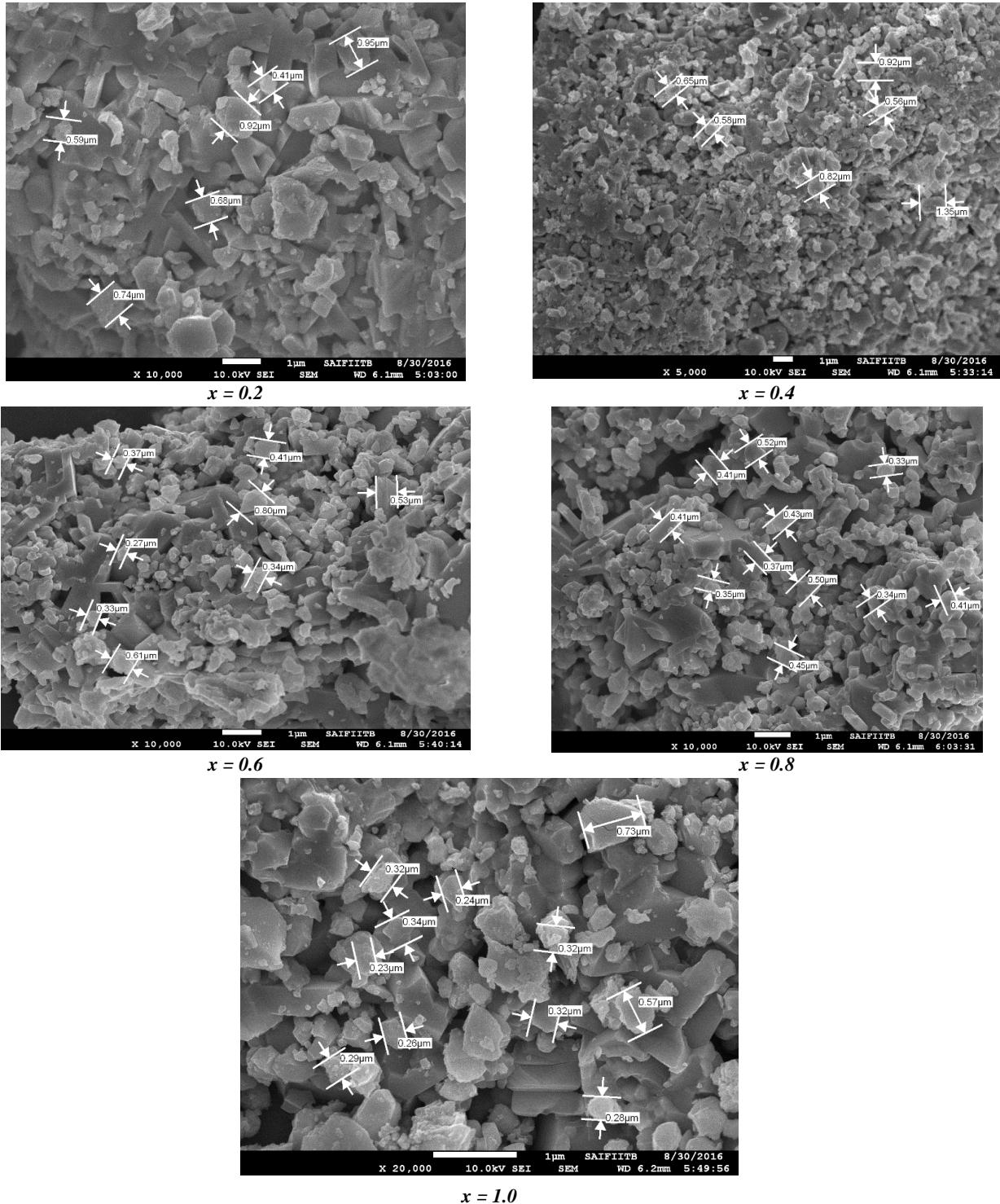


Fig. 2. Scanning electron micrographs of ferrite $\text{Ba}_{0.5}\text{Sr}_{0.5}\text{Co}_x\text{La}_x\text{Fe}_{12-2x}\text{O}_{19}$ with compositions ($0.0 \leq x \leq 1$ with steps of $x=0.2$)

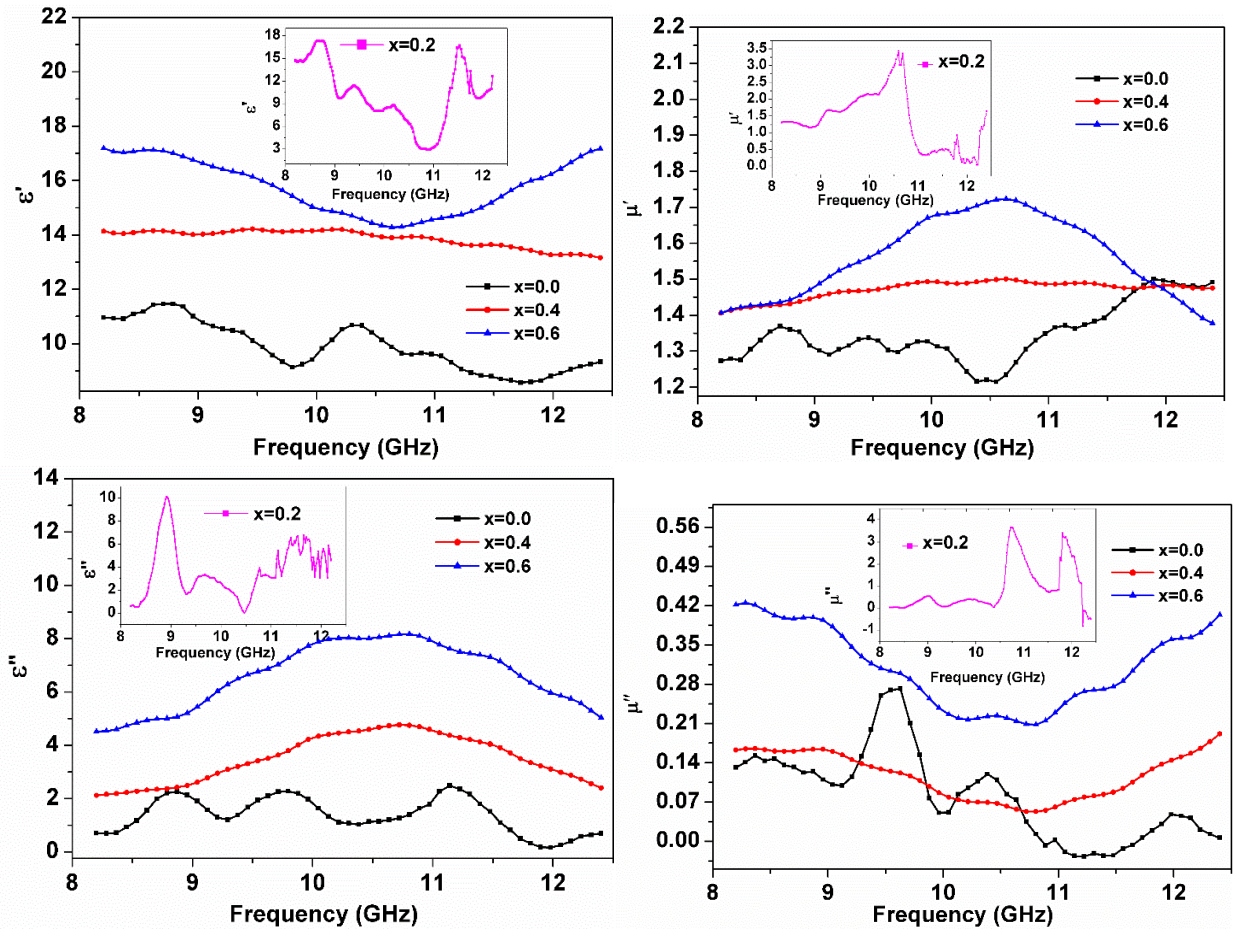


Fig. 3. Variations in complex permittivity, permeability, dielectric, and magnetic loss for different samples ferrite $Ba_{0.5}Sr_{0.5}Co_xLa_{1-x}Fe_{12-2x}O_{19}$ with compositions ($0.0 \leq x \leq 0.6$ with steps of $x=0.2$) (color online)

The large dispersion is examined in μ' and μ'' from frequency region 8.2–12.4 GHz. The maximum μ' is observed in $x = 0.2$ along the middle frequency region

while $x = 0.0$ remains at the lowest value along with all frequency range. The doping of Co^{2+} and La^{3+} bases a non-linear increase in μ' and μ'' of the compositions.

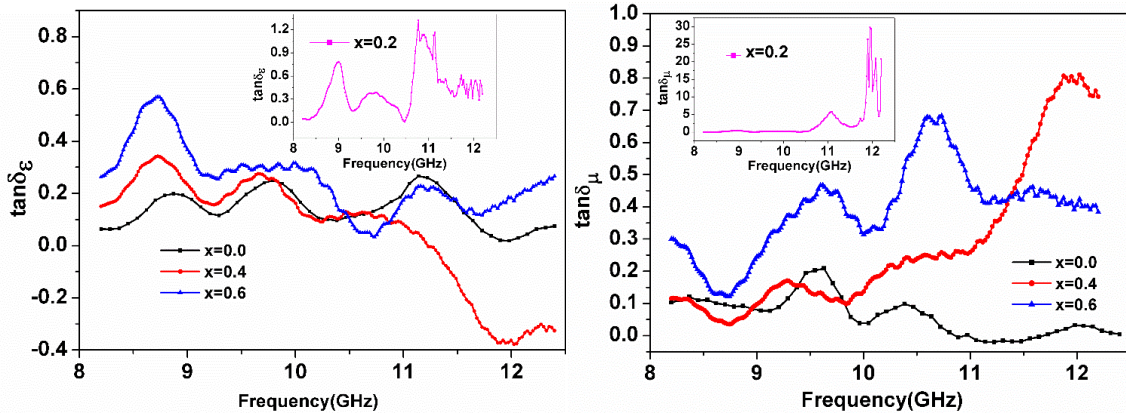


Fig. 4. Variations in dielectric & magnetic loss tangent for different samples ferrite $Ba_{0.5}Sr_{0.5}Co_xLa_{1-x}Fe_{12-2x}O_{19}$ with compositions ($0.0 \leq x \leq 0.6$ with steps of $x=0.2$) (color online)

Moreover, the ratio of dielectric loss to value of dielectric constant is called as dielectric loss tangent which is expressed as $\tan\delta_\epsilon = \epsilon''/\epsilon'$. Also, the proportionality of magnetic loss to permeability is called as magnetic loss

tangent expressed with $\tan\delta_\mu = \mu''/\mu'$. Moreover, absorption is dependent on these loss tangents. Fig. 4 shows these loss tangents $\tan\delta_\epsilon$ and $\tan\delta_\mu$ for different values of compositions and the major peaks of magnetic

loss as compared to dielectric loss which shows that higher absorption is achieved with magnetic loss. The nearness within dielectric loss tangent and magnetic loss tangent enhances impedance matching and also increases microwave frequency absorption.

3.2.2. Mechanism of quarter wavelength ($\lambda/4$)

If ferrite thickness is same as an odd multiple of wavelength ($n\lambda/4$), (n can be 1, 3, 5, 7, 9.....) of microwave frequency, then this frequency signal will be absorbed while traveling through the material.

Ferrite thickness is expressed as:

$$t = n/4 = (n.c)/4f|\mu_r \epsilon_r|^{1/2} \quad (1)$$

In the above expression, symbol 't' is used for matching thickness, 'c' is used for velocity of light, 'f_m' is used for matching frequency, and also n is an odd integer. Also, $\mu_r = \mu' - j\mu''$, $\epsilon_r = \epsilon' - j\epsilon''$ which are expressed in the experimental procedure.

The transmission line study explains reflection loss (RL) with input impedance (Z_{in}) to express microwave absorption in detail. High microwave absorption is related to the high value of reflection loss (RL). It can be formulated as given below:

$$RL \text{ (reflection loss)} = 20 \log |(Z_{in} - Z_0) / (Z_{in} + Z_0)| \quad (2)$$

In the above expression, Z_0 is called as the free space characteristic impedance and its value is 377Ω & metal-backed absorber's input impedance is represented by Z_{in} , which can be expressed as,

$$Z_{in} = Z_0 (\mu_r / \epsilon_r)^{1/2} \tanh [j(2\pi ft/c) (\mu_r \cdot \epsilon_r)^{1/2}] \quad (3)$$

$Z_{in} = Z_0$ is the condition of impedance matching and for ideal absorption, condition $Z_{in}/Z_0=1$ should be satisfied. Microwave absorption has been examined from the graph of RL for different values of simulation thickness along with frequency.

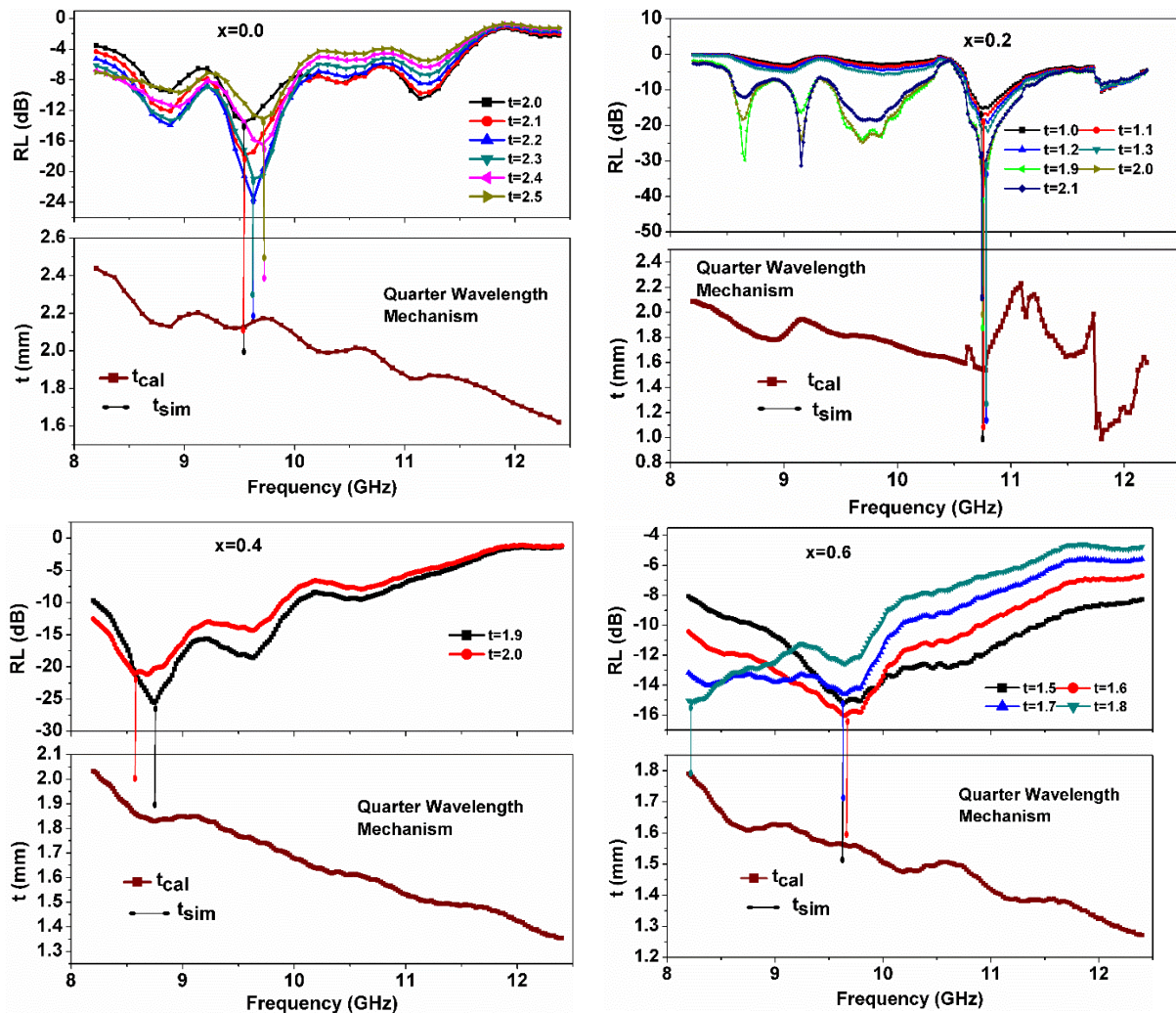


Fig. 5. Reflection Loss analysis w.r.t frequency of ferrite $Ba_{0.5}Sr_{0.5}Co_xLa_xFe_{12-2x}O_{19}$ with compositions ($0.0 \leq x \leq 0.6$ with steps of $x=0.2$) (color online)

The peaks of reflection loss with composition $x=0.0$ are at the same frequency i.e 9.71GHz for $t=2.4$ and 2.5 mm. Similarly for 2.2 and 2.3 mm, peaks occur at 9.62 GHz, and for 2.0 and 2.1 mm, RL peaks occur at 9.54 GHz frequency. For $x=0.2$, the maximum RL peaks are present at 10.75 GHz frequency for $t=1.0, 1.1, 1.9, 2.0$, and 2.1 mm and for $t=1.2$ and 1.3 mm, RL dips occur at 10.79 GHz. But for $x=0.4$ as we move towards the small frequency range thickness increases. For $t=1.9$ mm, RL is maximum at 8.74 GHz and for $t=2.0$, it is at 8.67 GHz. This is related with the quarter-wavelength mechanism given in equation (1) which describes an inverse relationship among frequency and thickness of material. For $x=0.6$, RL occurs at 9.63 GHz for $t=1.5$ and 1.7mm, for $t=1.6$, it occurs at 9.65 GHz and for $t=1.8$, peaks occurs at 8.23GHz. The highest value of reflection loss (RL) is -43.73 dB with composition $x=0.2$ at frequency of 10.75 GHz and sample thickness of 1.9 mm. Then, to find the relation of RL and mechanism of quarter wavelength, evaluation of calculated thickness (t_{cal}) is performed by equation (1), then compared to a simulated thickness (t_{sim}) through which RL can be calculated using equation (2). Fig. 5 show calculated thickness or $n\lambda/4$ graphs related to frequency: curves of calculated thickness are generated using $n=1$ in equation (1). To compare the calculated thickness and simulated thickness for peaks of reflection loss, lines in vertical form are drawn through the highest values of reflection loss to calculated thickness graphs. Simulated thickness is represented by bubbles on graphs for reflection loss values.

It is noticeable through Fig. 5 that the bubble with a line in vertical form, drag by maximum reflection loss peaks for the described simulated thickness, exists nearby calculated thickness, shown on $n\lambda/4$ curve. Thus with compositions $x=0.0, 0.2, 0.4$ and 0.6, reflection loss values higher than -10dB and -20 dB represent a mechanism of quarter wavelength with calculated thickness and simulated thickness. For $x=0.0, 0.2, 0.4$ and 0.6, it is shown that for maximum RL, the calculated

(2.15, 1.54, 1.82, 1.56mm) and simulated thicknesses (2.2, 1.9, 1.9, 1.6mm) respectively are approximately equal.

3.2.3. Matching among characteristic impedance and absorber impedance

The representation of the change in RL and $|Z_{in}|$ related to frequency is given in Fig. 6 with distinct values of a complex quantity which is expressed as $Z_{in} = Z_{real} + Z_{img}$ where Z_{real} is real part of input impedance and Z_{img} is imaginary part of input impedance. According to equation (2), a higher value of RL is obtained if $|Z_{in}|$ and Z_o are approximately equal and also equal to 377Ω , it will happen when Z_{real} is near to 377Ω and Z_{img} is near to 0Ω : As Z_{real} increases or decreases and or Z_{img} is positive/negative, RL starts decreasing accordingly. If Z_{in} and Z_o are approximately equal then RL will be higher. For good representation, Z_o is plotted by a horizontal line on curves RL and $|Z_{in}|$. The Microwave absorption will be higher when $|Z_{in}|$ closes to 377Ω . This condition is satisfied and RL peaks are displayed by distinct compositions.

For composition $x=0.2$, maximum RL is recorded as -43.73 at frequency 10.75 GHz and at this frequency, Z_{real} & Z_{img} observed as 381.90 & 0.56 respectively. It satisfies the impedance matching condition. Besides that for other compositions $x=0.0, 0.4$ and 0.6, we are acquiring satisfied values of RL as -23.61, -25.58 & -16.01 dB at 9.62, 8.74 & 9.65 GHz frequencies respectively. But it can be seen from the graphs that for these compositions Z_{in} and Z_{real} values are not closed to 377Ω and 0Ω respectively. So, we can say that for the remaining compositions criterion of Impedance matching is not obeyed.

Despite this, high values of magnetic loss and magnetic loss tangent have been explained earlier for these compositions. Thus, for composition $x=0.2$, there is more contribution of impedance matching to provide microwave absorption.

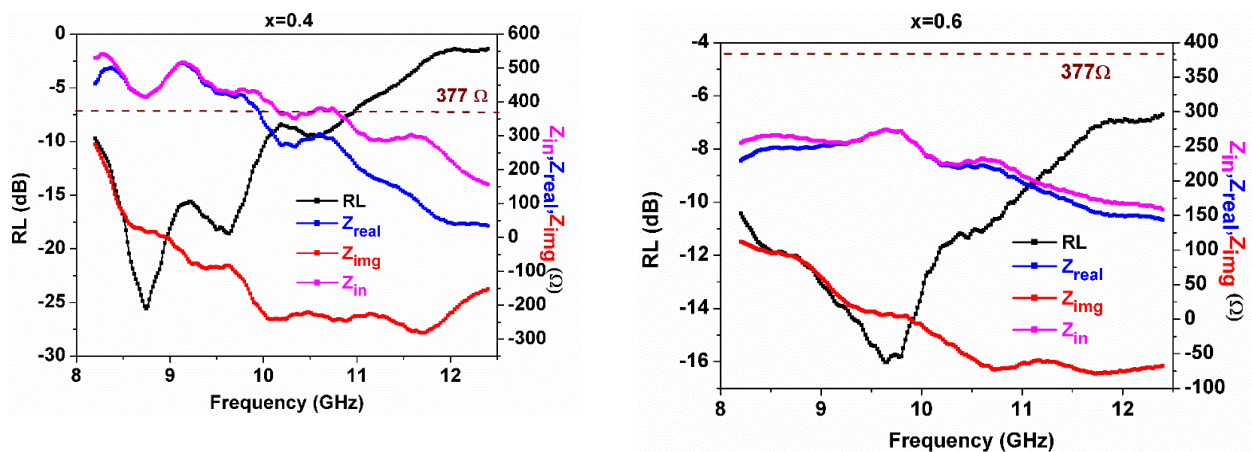


Fig. 6. Impedance matching for ferrite $Ba_{0.5}Sr_{0.5}Co_3La_3Fe_{12-2x}O_{19}$ with compositions ($0.0 \leq x \leq 0.6$ with steps of $x=0.2$) (color online)

For the same synthesized material, it is also observed that this material can be used as good absorber in all possible applications either these are of wideband or narrowband in nature. As the case of composition $x=0.2$ it has maximum RL as -43.73dB and it offers B.W (0.07GHz) as narrowband with $-10\text{dB}\leq\text{RL}\leq-20\text{dB}$ & B.W (0.2GHz) with $\text{RL}\geq-20\text{dB}$. Similarly the composition $x=0.6$ offers the wideband response of B.W of 2.7GHz with $10\text{dB}\leq\text{RL}\leq-20\text{dB}$ and having maximum RL as -16.01dB at frequency 9.65GHz. It can also be observed that we can vary the band as per the requirement with varying composition and varying the thickness values too.

4. Conclusions

In this paper, M-type hexagonal ferrite $\text{Ba}_{0.5}\text{Sr}_{0.5}\text{Co}_x\text{La}_x\text{Fe}_{12-2x}\text{O}_{19}$ was synthesized with ($0.0\leq x\leq 1$ with steps of $x=0.2$) compositions using the standard ceramic method. Composition $x=0.2$ examined better characteristics of microwave frequency absorption among the demonstrated frequency region, so it will be used for wideband and or narrowband applications. Moreover, the reasons for best signal absorption with $x=0.2$ are the quarter wavelength measures, impedance matching, deviation among $\tan\delta_{\mu}$ and $\tan\delta_{\epsilon}$, and microstructural design. The demonstrated methods can be utilized to obtain optimized absorption in the microwave frequency region, to evaluate frequency and thickness in mm for achieving maximum absorption in the microwave frequency range and in developing microwave absorbers.

References

- [1] K. Mukherjee, S.B. Majumder, *Sensors and Actuators B: Chemical* **162** (1), 229 (2012).
- [2] S. Padhy, S. Sanyal, R.S. Meena, R. Chatterjee, A. Bose, *IET Microwaves, Antennas and Propagation* **8**(3), 165 (2014).
- [3] H. Kaur, C. Singh, R. Kaur, T. Dhiman, S. B. Narang, *The European Physica, J. B* **88**, 274 (2015).
- [4] A. Septiani, T. Kristiantoro, Dedi, N. Idayanti, Y. Taryana, *ICRAMET, Jakarta*, 149 (2016).
- [5] C. Singh, R. Kaur, S.B. Narang, M. Puri, T. Dhiman, H. Kaur, *Journal Electron. Mater.* **45**, 4908 (2016).
- [6] S. S. S. Afghahi, M. Jafarian, & Y. Atassi, *J. Nanopart. Res.* **18**, 192 (2016).
- [7] E. Handoko, I. Sugihartono, M. A. Marpaung, Z. Jalil, M. Randa, C. Kurniawan, M. Alaydrus, *International conference on broadband communication, wireless sensors and powering (BCWSP)*, Jakarta, 1 (2017).
- [8] R. Topkaya, *Appl. Phys. A* **123**, 488 (2017).
- [9] S. Mortazavinik, M. Yousefi, *Russ. J. Appl. Chem.* **90**, 298 (2017).
- [10] S. Padhy, A. De, R. R. Debata, R. S. Meena, *IEEE Transactions on Electromagnetic Compatibility* **60**(6), 1734 (2018).
- [11] A. Arora, S.B. Narang, *Journal Electron. Mater.* **47**, 4919 (2018).
- [12] P. J. Liu, Z. J. Yao, V. M. H. Ng, J. T. Zhou, Z. H. Yang, L. B. Kong, *Acta Metall. Sin. (Engl. Lett.)* **31**, 171 (2018).
- [13] I. Araz, F. Genç, *J Supercond, Nov. Magn.* **31**, 279 (2018).
- [14] A. Septiani, H. I. Sanjaya, Dedi, *ICRAMET, Tangerang, Indonesia*, 131 (2019).
- [15] P. Intaphong, N. Radkhaochatsain, W. Somraksa, S. Musigawon, N. Kongthong, R. Kaemkit, S. Samadoloh, T. Chanadee, *Current Applied Physics* **19**(4), 548 (2019).
- [16] D. P. Dubey, S. Kumar, R. Chatterjee, *Physica B: Condensed Matter* **570**, 19 (2019).
- [17] J-H. You, S. Choi, S-Y. Park, S. I. Yoo, *Journal of Magnetism and Magnetic Materials* **491**, 165640 (2019).
- [18] P. Azizi, S. M. Masoudpanah, S. Alamolhoda, *Appl. Phys. A* **125**, 686 (2019).
- [19] M. B. Shelar, S. N. Yadav, *Int. J. Self-Propag. High-Temp. Synth.* **28**, 173 (2019).
- [20] R. Peymanfar, S. Javanshir, M. R. Naimi-Jamal, A. Cheldavi, M. Esmkhani, *Journal Electron. Mater.* **48**, 3086 (2019).
- [21] T. Y. Kiseleva, E. V. Lazareva, S. I. Zholudev, T. F. Grigoreva, E. T. Devyatkina, I. P. Ivanenko, E. V. Yakuta, A. S. Ilyushin, N. Z. Lyakhov, *Materials Today, Proceedings* **25**, 513 (2020).
- [22] A. V. Trukhanov, K. A. Astapovich, M. A. Almessiere, V. A. Turchenko, E. L. Trukhanova, V. V. Korovushkin, A. A. Amirov, M. A. Darwish, D. V. Karpinsky, D. A. Vinnik, D. S. Klygach, M. G. Vakhitov, M. V. Zdorovets, A. L. Kozlovskiy, S. V. Trukhanov, *Journal of Alloys and Compounds* **822**, 153575 (2020).
- [23] P. N. Dhruv, S. S. Meena, R. C. Pullar, F. E. Carvalho, R. B. Jotania, P. Bhatt, C. L. Prajapat, J. P. B. Machado, T. V. C. Rao, C. B. Basak, *Journal of Alloys and Compounds* **822**, 153470 (2020).
- [24] M. Jafarian, S. S. S. Afghahi, Y. Atassi, Y. A. Loriani, *Journal of Magnetism and Magnetic Materials* **493**, 165680 (2020).
- [25] H. Kaur, A. Marwaha, A. C. Singh, S. B. Narang, R. Jotania, Y. Bai, S. R. Mishra, D. Singh, A. S. B. Sombra, M. Ghimire, P. Dhruv, *Journal Electron. Mater.* **49**, 1646 (2020).
- [26] A. Garg, S. Goel, N. Kumari, A. Dubey, N. E. Prasad, S. Tyagi, *Journal Electron. Mater.* **49**, 2233 (2020).
- [27] S. R. S. Afshar, S. M. Masoudpanah, M. Hasheminasari, *Journal of Electronic Materials* **49**(3), 1742 (2020).
- [28] P. Kaur, S. Bahel, S. B. Narang, *Journal Electron. Mater.* **49**, 1654 (2020).
- [29] M. Fathi, M. M. Mehdipour, H. Shokrollahi, *J. Aust. Ceram. Soc.* **56**, 251 (2020).
- [30] L. T. Q. Anh, N. V. Dan, *Appl. Phys. A* **126**, 67 (2020).
- [31] H. Kaur, A. Marwaha, C. Singh, S. B. Narang, R. Jotania, S. Jacobo, A. S. B. Sombra, S. V. Trukhanov, A. V. Trukhanov, P. Dhruv, *Journal of Alloys and Compounds* **806**, 120 (2019).

*Corresponding author: er.harsimrat@gmail.com